Gpr158 mediates osteocalcin's regulation of cognition

Lori Khrimian,[1]* Arnaud Obri,[1]* Mariana Ramos-Brossier,[4,5,6] Audrey Rousseaud,[4,5,6] Stéphanie Moriceau,[4,5,6] Anne-Sophie Nicot,[7,8] Paula Mera,[1] Stylianos Kosmidis,[2,9,11] Theodoros Karnavas,[1] Frederic Saudou,[7,8,12] Xiao-Bing Gao,[13] Franck Oury,[4,5,6] Eric Kandel,[2,3,10,11] and Gerard Karsenty[1]

[1]Department of Genetics and Development, [2]Department of Neuroscience, and [3]Kavli Institute for Brain Science, Columbia University Medical Center, New York, NY
[4]Institut Necker-Enfants Malades, CS 61431, Paris, France
[5]Institut National de la Santé et de la Recherche Médicale, U1151, Paris, France
[6]Université Paris Descartes, Sorbonne Paris Cité, Paris, France
[7]Grenoble Institute des Neurosciences, Université Grenoble Alpes, Grenoble, France
[8]INSERM, U1216, Grenoble, France
[9]Howard Hughes Medical Institute and [10]Zuckerman Mind Brain Behavior Institute, Columbia University, New York, NY
[11]New York State Psychiatric Institute, New York, NY
[12]CHU Grenoble Alpes, Grenoble, France
[13]Program in Integrative Cell Signaling and Neurobiology of Metabolism, Section of Comparative Medicine, Yale University School of Medicine, New Haven, CT

That osteocalcin (OCN) is necessary for hippocampal-dependent memory and to prevent anxiety-like behaviors raises novel questions. One question is to determine whether OCN is also sufficient to improve these behaviors in wild-type mice, when circulating levels of OCN decline as they do with age. Here we show that the presence of OCN is necessary for the beneficial influence of plasma from young mice when injected into older mice on memory and that peripheral delivery of OCN is sufficient to improve memory and decrease anxiety-like behaviors in 16-mo-old mice. A second question is to identify a receptor transducing OCN signal in neurons. Genetic, electrophysiological, molecular, and behavioral assays identify *Gpr158*, an orphan G protein–coupled receptor expressed in neurons of the CA3 region of the hippocampus, as transducing OCN's regulation of hippocampal-dependent memory in part through inositol 1,4,5-trisphosphate and brain-derived neurotrophic factor. These results indicate that exogenous OCN can improve hippocampal-dependent memory in mice and identify molecular tools to harness this pathway for therapeutic purposes.

INTRODUCTION

Osteocalcin (OCN) is a multipurpose bone-derived hormone (Karsenty and Olson, 2016). In particular, OCN crosses the blood–brain barrier, binds to neurons in specific brain regions, prevents neuronal apoptosis in the hippocampus, favors the synthesis of all monoamine neurotransmitters, and inhibits that of gamma-aminobutyric acid. These cellular and molecular functions may explain why OCN is necessary for hippocampal-dependent memory and to reduce anxiety-like behaviors (Oury et al., 2013). The severity of the cognitive deficit noted in any mouse model lacking a hormone synthesized in a peripheral organ, such as OCN, brings up several questions.

One question raised by the cognitive defects seen in *Ocn*−/− mice, and by the fact that circulating levels of OCN plummet early in the life of all species (Chiappe et al., 1999; Mera et al., 2016), is to determine whether pathological conditions developing over time in adult animals that also affect physiological processes regulated by OCN could be secondary, in part, to this plummet in circulating OCN levels. Hippocampal-dependent memory is one such physiological process. The ability of plasma from young mice to improve cognitive function when injected into older mice (Villeda et al., 2014) and the availability of *Ocn*−/− mice provide necessary tools to begin addressing this question. A complementary approach to answering this question is to assess whether peripheral delivery of exogenous OCN is sufficient to improve the deficit in cognitive functions seen in older WT mice. A second question, of mechanistic and translational nature, is to elucidate OCN's mode of action in the brain. This requires identifying a receptor that transduces OCN signal in the brain regions where it binds.

Addressing the first question, we show here that injections of plasma from young mice into older mice can improve their cognitive function only if the plasma contains OCN and that exogenous OCN is sufficient to correct the decline in cognitive function observed in older mice. Addressing the

*L. Khrimian and A. Obri contributed equally to this paper.

Correspondence to Gerard Karsenty: gk2172@cumc.columbia.edu

Abbreviations used: ACSF, artificial cerebrospinal fluid; AP, action potential; BDNF, brain-derived neurotrophic factor; BW, body weight; EPMT, elevated plus maze test; fEPSP, field excitatory postsynaptic potential; GPCR, G protein–coupled receptor; IP3, inositol 1,4,5-trisphosphate; LTP, long-term potentiation; MF, mossy fiber; NOR, novel object recognition; OCN, osteocalcin; OFT, open field test; TIMP, tissue inhibitor of metalloproteinases.

The Rockefeller University Press
J. Exp. Med. 2017 Vol. 214 No. 10 2859–2873
https://doi.org/10.1084/jem.20171320

second question, we provide expression, genetic, electrophysiological, molecular, and functional evidence that the orphan class C G protein–coupled receptor (GPCR) Gpr158 mediates OCN's regulation of cognitive function. Together, these data pave the way to test whether OCN signaling in the brain could be harnessed to combat cognitive decline.

RESULTS AND DISCUSSION

To determine whether OCN is a necessary component of plasma from young mice, contributing to its beneficial effect on cognition in older mice, we relied on the novel object recognition (NOR) test, which evaluates hippocampal-dependent memory because this task is altered in *Ocn*−/− mice (Oury et al., 2013). 16-mo-old WT mice had a significant defect in hippocampal-dependent memory compared with 3-mo-old (young) WT mice. This cognitive defect was significantly improved when plasma from young mice was injected into 16-mo-old mice but not when plasma from other 16-mo-old WT mice was injected in 16-mo-old WT littermates (Fig. 1 A). Because OCN limits anxiety-like behavior (Oury et al., 2013), we also subjected young and 16-mo-old mice to the elevated plus maze test (EPMT), which assesses anxiety-like behavior as a shorter time spent in the open arms and fewer number of entries in the open arms (Crawley, 1985). We found that plasma from young mice, when injected into 16-mo-old mice, significantly reduced anxiety-like behaviors (Fig. 1 B).

In contrast, when plasma from young *Ocn*−/− mice was injected into 16-mo-old WT mice, there was no improvement of hippocampal-dependent memory or anxiety-like behaviors in the recipient mice (Fig. 1, A and B; and Fig. S1 A). The inability of the plasma from young *Ocn*−/− mice to improve cognition in older mice was not explained by an increase in β_2 microglobulin accumulation, a progeronic molecule in this plasma (Smith et al., 2015; Fig. S1 B). To further demonstrate that the presence of OCN is necessary for the beneficial effect of plasma from young mice on cognition when injected into 16-mo-old WT mice, we performed two experiments. First, we used plasma obtained from young *Ocn*−/− mice that had been supplemented with mouse recombinant uncarboxylated OCN (spiked plasma). We first verified that injections of spiked plasma increased circulating OCN levels in 16-mo-old WT mice (Fig. S1 C). Remarkably, injections of spiked plasma in 16-mo-old WT mice resulted in the same improvement in hippocampal-dependent memory that is achieved by injections of plasma from 3-mo-old WT mice (Fig. 1, A and B). This beneficial effect of the spiked plasma on cognitive function was not explained by a change in the accumulation of tissue inhibitor of metalloproteinases 2 (TIMP2) in the hippocampus, a molecule implicated in the beneficial effect of young plasma on cognition (Castellano et al., 2017; Fig. 1 C). Consistent with the beneficial effect of young plasma injections into older mice, injections of spiked plasma significantly reduced anxiety-like behaviors in 16-mo-old WT mice (Fig. 1, A and B). Second, we used an anti-OCN antibody to deplete OCN from the plasma of young WT mice. We verified before injection of this immune-depleted plasma that OCN content was decreased by 90% (Fig. S1 D). In a mirror image of what was observed when using spiked plasma, immune-depleted plasma from WT mice failed to increase hippocampal memory and to reduce anxiety to the same extent as control plasma (Fig. 1, D and E). Together, these experiments indicate that OCN is a necessary contributor to the beneficial effect of plasma from young WT mice on hippocampal-dependent memory and anxiety-like behaviors in older WT mice.

The steep decrease in circulating OCN levels before 1 yr of age (Fig. S1 E), and the crucial contribution of OCN to the beneficial effect of plasma from young mice on cognitive function of older mice, prompted us to test whether exogenous OCN would be sufficient to improve cognition in older mice. This was addressed by delivering OCN peripherally and continuously through minipumps for 2 mo in 14-mo-old WT mice because this hormone crosses the blood–brain barrier (Oury et al., 2013). This mode of administration substantially increased circulating OCN levels (Fig. S1 F). When tested for NOR, 16-mo-old WT mice that had received OCN continuously for 2 mo displayed a hippocampal-dependent memory that was similar to that of 3-mo-old WT mice (Fig. 1 F). The same improvement was observed when memory was analyzed through the Morris water maze test, which assesses spatial learning and memory in rodents (Nakazawa et al., 2002; Fig. 1 G). Similar results were observed in 12-mo-old WT mice (Fig. S1, G and H). In agreement with the notion that OCN regulates anxiety-like behaviors, chronic delivery of OCN improved anxiety-like behaviors as assayed by the EPMT in 12- and 16-mo-old WT mice (Oury et al., 2013; Fig. 1 H and Fig. S1 I).

The fact that OCN is necessary for the maintenance, and sufficient for the restoration, of cognitive function in older mice underscored the importance of identifying a receptor for this hormone in the brain because Gprc6a, OCN's receptor in peripheral organs (Karsenty and Olson, 2016), does not mediate OCN's functions in the brain (Oury et al., 2013). The bell-shaped curve of OCN signaling in brainstem explants (Oury et al., 2013) suggested that, as in the case of Gprc6a, the receptor for OCN in the brain might be a GPCR. We used three criteria to identify an orphan GPCR capable of transducing OCN signal in the brain.

The first criterion was that this orphan GPCR should belong to the same subfamily of GPCRs as Gprc6a, the class C subfamily. Second, this *Gpcr* should be expressed in the CA3 region of the hippocampus where OCN binds (Oury et al., 2013), and third, this *Gpcr* should not be expressed in cell types where OCN's signal is transduced through Gprc6a (Fig. 2 A). Using this approach, we identified one orphan class C GPCR, *Gpr158*, as being robustly expressed in neurons of the CA3 region of the hippocampus but not in any *Gprc6a*-expressing cells in peripheral tissues (Fig. 2, B and D; and Fig. S2, A and C). Gpr158 is present in *Map2*-expressing

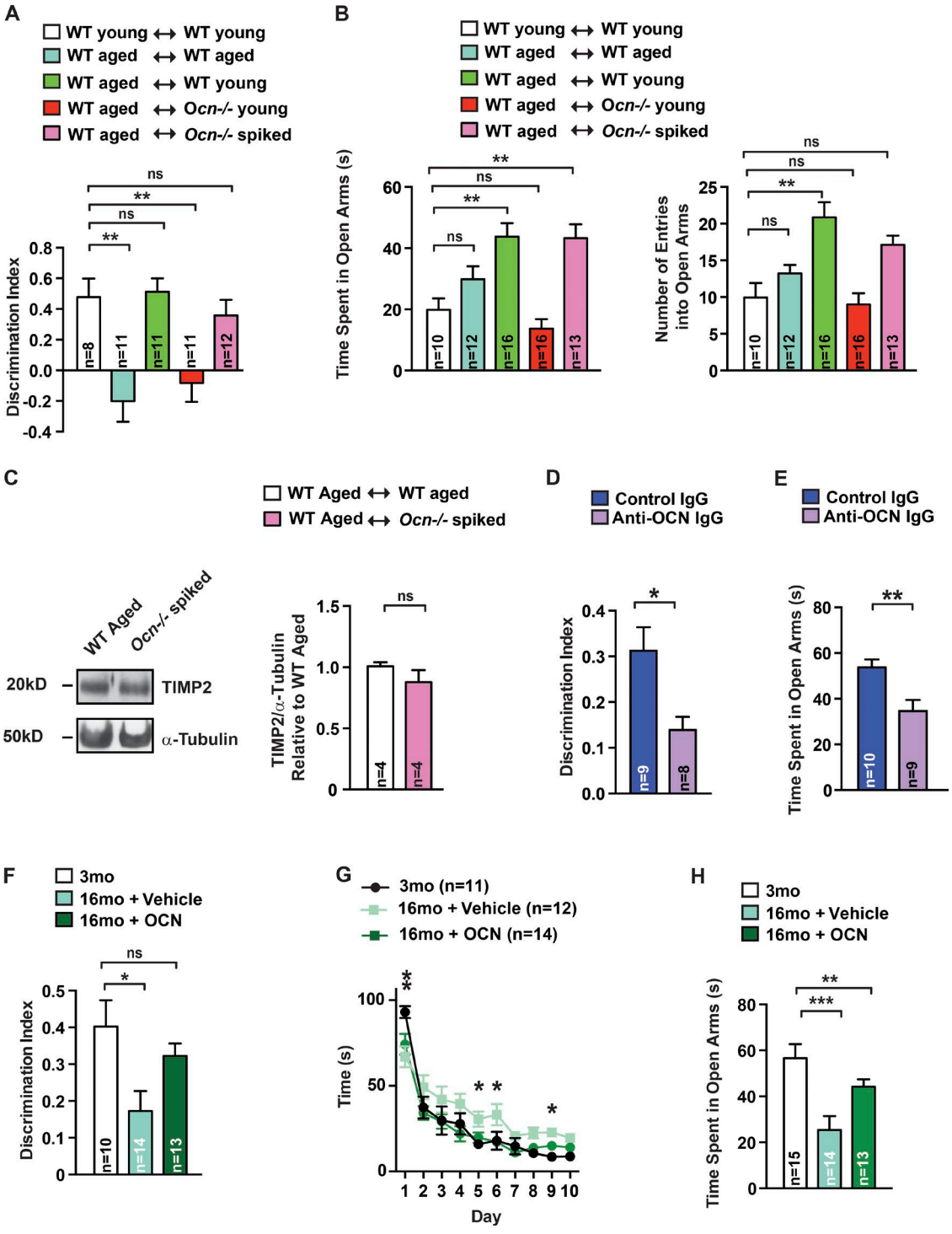

Figure 1. **OCN is sufficient to improve cognitive function and anxiety-like behaviors.** (A and B) NOR (A) and EPMT (B) performed in 3-mo-old (young) WT mice treated with plasma from young WT mice (n = 8–10) or 16-mo-old (aged) WT mice treated with plasma from WT mice, either aged (n = 11–12) or young (n = 11–16), or from young *Ocn*−/− mice (n = 11–16), or plasma from young *Ocn*−/− mice supplemented with 90 ng/g BW of OCN (spiked; n = 12–13). For NOR, discrimination index was measured; for EPMT, number of entries and time spent in the open arms were scored (one-way ANOVA followed by a Bonferroni post hoc test compared with WT young). (C) TIMP2 accumulation (representative Western blot, left) and quantification of band intensities (right) in hippocampi of older WT mice receiving plasma from *Ocn*−/− mice supplemented with 90 ng/g BW of OCN (Student's t test, n = 4 mice per group). α-Tubulin is used as a loading control. (D and E) NOR (D) and EPMT (E) performed in 18-mo-old mice treated with IgG (n = 9–10) or anti-Ocn immunodepleted plasma (n = 8–9). For NOR, discrimination index was measured. For EPMT, number of entries and time spent in the open arms were scored

pyramidal neurons from the CA3 region of the hippocampus but not in *Gfap*-expressing astrocytes in vivo (Fig. 2 F and Fig. S2 D). Similar results were obtained in cultured hippocampal cells using a specific antibody against Gpr158 (Fig. 2 G and Fig. S2 E). Adding credence to the notion that Gpr158 may be an OCN receptor, its accumulation was higher in *Ocn*−/− than in WT hippocampi, circulating OCN levels were twofold higher in *Gpr158*−/− compared with WT littermates, and local delivery of OCN in the anterior hippocampus induced c-Fos accumulation in neurons of the CA3 region in WT but not in *Gpr158*−/− mice (Fig. 2, H–J; and Fig. S2 F). A systematic analysis of its expression by in situ hybridization showed that *Gpr158* is also expressed in the somatosensory, motor, and auditory areas of the cortex, the piriform cortex, the retro-splenial area, and the ventral tegmental area (Fig. 2 E). A signaling pathway recruited by GPR158 was identified by a pull-down assay performed on solubilized membranes obtained from *Ocn*−/− hippocampi. In the conditions of this assay, biotin-labeled OCN bound a complex containing Gpr158 and Gαq (Fig. 2 K). The amount of Gαq pulled down was greatly reduced when membranes from *Gpr158*−/− hippocampi were used to perform this assay (Fig. 2 K). Consistent with the presence of Gαq in this complex, OCN increased the production of inositol 1,4,5-trisphosphate (IP3) significantly more in WT than *Gpr158*−/− hippocampal neurons (Fig. 2 L) and failed to increase in cAMP production (Fig. S2 H).

We used behavioral and electrophysiological assays to assess whether Gpr158 mediates OCN's regulation of cognitive function. Using NOR, we observed that mice lacking *Gpr158* in the forebrain only had a deficit in hippocampal-dependent memory, as *Gpr158*−/− mice did. This deficit, however, was less severe in $Gpr158_{CamkIIa}$−/− than in *Gpr158*−/− mice (Fig. 3 A and Fig. S3, A–D), most likely because of the low efficiency of *Gpr158* deletion using *CamkIIa-Cre* mice (Fig. S3 D). Hence, we used *Gpr158*−/− mice for the rest of the experiments. Because the deficit observed in the Morris water maze test was less severe in *Gpr158*−/− mice than what was reported in *Ocn*−/− mice (Fig. 3 B), we performed three additional experiments to establish that Gpr158 mediates OCN's ability to favor hippocampal-dependent memory. First, we delivered OCN peripherally and continuously through minipumps for 1 mo in *Gpr158*−/− mice before testing. This delivery of OCN failed to rescue the cognitive defect observed in *Gpr158*−/− mice (Fig. 3 C and Fig. S3 E). Second, we injected lentivirus expressing either shRNA targeting *Gpr158*, which resulted in a >60% decrease in Gpr158 protein levels, or scrambled shRNA as a control, in the dorsal hippocampus of 3-mo-old WT male mice (Fig. S3 F). Ten days later, OCN was injected at the same stereotaxic coordinates. We found that local delivery of OCN significantly improved hippocampal-dependent memory in control mice but not in mice in which Gpr158 accumulation had been efficiently down-regulated (Fig. 3 D). A similar result was observed when mice were subjected to contextual fear conditioning, which measures associative memory and requires the integrity of the hippocampus (Saxe et al., 2006; Denny et al., 2012; Fig. 3 E). Third, we analyzed compound heterozygous mice (*Gpr158*+/−;*Ocn*+/−). Whereas single heterozygous mice did not display any measurable abnormalities in the NOR, *Gpr158*+/−;*Ocn*+/− mice behaved similarly to *Gpr158*−/− or *Ocn*−/− mice (Fig. 3 F).

To add support to the notion that Gpr158 mediates OCN's regulation of cognitive functions, we performed electrophysiological studies in WT and *Gpr158*−/− cells. In whole-cell current-clamp recordings, we found that OCN enhanced action potential (AP) frequency in pyramidal cells of the CA3 region of WT but not *Gpr158*−/− hippocampi (Fig. 3 G and Fig. S3 G). Consistent with the observation that Gpr158 forms a complex with Gαq, 2-aminoethoxydiphenyl borate, an IP3 receptor antagonist (Maruyama et al., 1997), nearly abolished OCN's ability to enhance AP frequency in pyramidal cells of the CA3 region (Fig. 3 H). Next, we examined long-term potentiation (LTP) expression in synapses from the mossy fiber (MF) to CA3 neurons using hippocampal slices from WT and *Gpr158*−/− mice. The field excitatory postsynaptic potentials (fEPSPs) recorded in the CA3 region by stimulating the MF cells could be blocked by the application of DCG-IV (Fig. S3 H). To verify LTP at the MF-CA3 pyramidal synapses (Kamiya et al., 1996), two trains of tetanic stimulation were applied to the MF-CA3 synapses after a stable baseline of fEPSPs were recorded. The tetanic stimulation induced a brief post-tetanic potentiation and LTP in WT (baseline, 106.5 ± 3.4%; 50 min after tetanus, 126.7 ± 10.1%; $P < 0.05$) but not in *Gpr158*−/− hippocampal slices (baseline, 100.9 ± 1.5%; 50 min after tetanus, 104.9 ± 6.8%; $P > 0.05$; Fig. 3 I). Of note, tetanic stimulation induced a brief depression but no potentiation right after the completion of the tetanus in *Gpr158*−/− slices.

Because OCN regulates anxiety-like behaviors, we subjected *Gpr158*−/− and WT littermates to the EPMT and the dark-to-light transition test, which measures anxiety-like behaviors on the basis of the innate aversion of rodents to brightly illuminated areas (Crawley, 1985). As in the case of *Ocn*+/− and *Ocn*−/− mice, anxiety-like behavior was increased in 3-mo-old *Gpr158*+/− and *Gpr158*−/− mice

(Student's *t* test). (F–H) NOR (F), Morris water maze test (MWMT; G), and EPMT (H) performed in 3-mo-old (n = 10–15) and older WT mice treated with saline (n = 12–14) or OCN (n = 13–14; 90 ng/h) for 2 mo. For NOR, discrimination index was measured (one-way ANOVA followed by a Bonferroni post hoc test compared with WT young). For MWMT, the graph shows the time to localize a submerged platform in the swimming area (two-way repeated-measures ANOVA followed by a Fisher's least significantly different post hoc test compared with 3 mo old). For EPMT, time spent in the open arms was measured (one-way ANOVA followed by a Bonferroni post hoc test compared with WT young). Results are given as mean ± SEM. *, $P \leq 0.05$; **, $P \leq 0.01$; ***, $P \leq 0.001$.

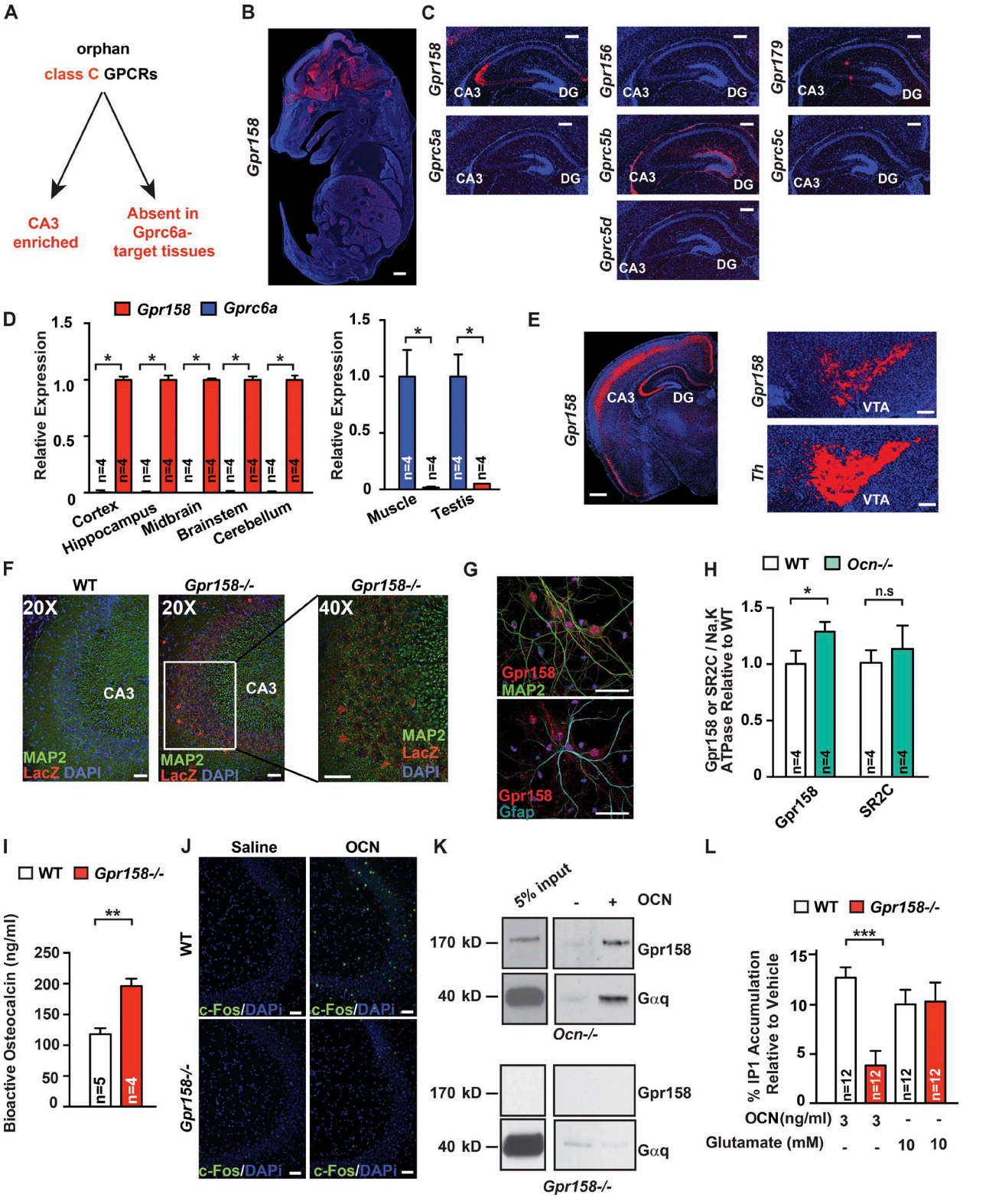

Figure 2. **Identification of a receptor for OCN in the brain.** (A) Strategy used to identify an OCN brain receptor. (B) In situ hybridization of *Gpr158* in E14.5 WT mouse embryos. Bar, 0.5 mm. (C) In situ hybridization of *Gpr158*, *Gpr156*, *Gpr179*, *Gprc5a*, *Gprc5b*, *Gprc5c*, and *Gprc5d* in the brain of 10-d-old WT mice. Bar, 200 µm. (D) Expression of *Gpr158* and *Gprc6a* in various tissues of 3-mo-old WT mice (Student's *t* test, $n = 4$ mice per group). In the brain-derived tissues, expression is relative to *Gpr158* expression, and in peripheral tissues, expression is relative to *Gprc6a*. (E) In situ hybridization of *Gpr158* in the brain of 3-mo-old WT mice. For the ventral tegmental area (VTA), *Th* was used as a positive control. Bar, 200 µm. (F) Immunofluorescence of Lacz and

(Fig. 3, J and K). In a third test, the open field test (OFT), which measures anxiety as a decrease in total ambulation and time spent in the center of the box, *Gpr158*+/− and *Gpr158*−/− mice displayed anxiety-like behaviors similar to *Ocn*+/− and *Ocn*−/− mice (Oury et al., 2013; Fig. 3, L and M). Additionally, the month-long peripheral delivery of OCN to *Gpr158*−/− did not reduce anxiety-like behavior in these mice (Fig. S3 I).

In trying to identify molecular events triggered by OCN through Gpr158, we asked whether OCN may act through brain-derived neurotrophic factor (BDNF) signaling, a molecular pathway critical for hippocampal-dependent memory, whose regulation by bone-derived signals has not yet been reported (Hall et al., 2000; Yamada and Nabeshima, 2003). For that purpose, we monitored the transport of BDNF-containing dense-core vesicles in embryonic rat neurons seeded in microchambers, and transduced with lentivirus, allowing the expression of BDNF-mCherry (Fig. 4 A). These neurons were left to differentiate for 9 to 11 d. Axons were imaged every 200 ms in microchannels to quantify kinetics of anterograde (from soma to synapse) and retrograde (from synapse to axon) transport of BDNF vesicles under control conditions or after 4 h of OCN treatment. OCN thus stimulates the global trafficking of BDNF vesicles and its specific transport to synapses, as shown by the increase in transport velocity of both anterograde and retrograde BDNF vesicles and the decrease in time spent in pause (Fig. 4 B). Moreover, the number of motile anterograde vesicles was larger (Fig. 4 B).

Several lines of evidence obtained using WT or Gpr158-null cells support the notion that BDNF is a mediator of OCN's functions in the brain. First, *Bdnf* expression was decreased in hippocampi and midbrains of *Gpr158*−/− mice (Fig. 4 C and Fig. S3 J) and OCN increased *Bdnf* expression significantly more in WT than in *Gpr158*−/− cultured hippocampal neurons (Fig. 4 D). Second, delivery of OCN increased the accumulation of BDNF in mice that had received scrambled shRNA but not in those in which Gpr158 abundance had been efficiently decreased by shRNA targeting *Gpr158* (Fig. 4, E and F). Third, peripheral delivery of OCN increased *Bdnf* expression in hippocampi of 16-mo-old WT mice (Fig. 4 G). Fourth, BDNF accumulation was increased in hippocampi of older WT mice receiving plasma from young WT mice but not in hippocampi of older mice receiving plasma from young *Ocn*−/− or from older WT mice (Fig. 4 H). Last, BDNF accumulation in the hippocampus was higher in 16-mo-old WT mice that had received plasma from *Ocn*−/− mice supplemented with OCN (Fig. 4 H).

The identification of extracellular cues favoring hippocampal-dependent memory, and the elucidation of their mechanism of action, is of utmost importance to understand how cognition is regulated and can be altered under pathological circumstances. At the same time, the identification of such molecules raises questions regarding their signaling in the brain. By showing that the bone-derived hormone OCN is sufficient to improve hippocampal-dependent memory in 16-mo-old mice, the results presented here underscore the importance of OCN in modulating these functions throughout life. That these effects of OCN signaling in the brain are independent of β_2 microglobulin and TIMP2 indicates that multiple circulating molecules, some of which are hormones, affect cognitive function (Villeda et al., 2014; Castellano et al., 2017). As a critically important molecular extension of this work, we show through several types of assays that OCN mediates its influence on cognitive function through its interaction with an orphan class C GPCR, Gpr158. The identification of a receptor, expressed in neurons of the hippocampal CA3 region that transduces OCN signal, paves the way to potentially use this pathway for therapeutic purposes. As important, because *Gpr158* is expressed in other regions of the brain besides the hippocampus, its identification as a receptor for OCN provides a much-needed tool to embark on a more extensive analysis of the functions OCN may have in the brain.

MATERIALS AND METHODS

Animals

For all experiments, we used females and littermates as controls unless otherwise stated. *Ocn*−/− (*osc*^{m1}/*osc*^{m1}) mice were generated by our laboratory and previously described (Ducy et al., 1996). *Gpr158*−/− (Gpr158$^{tm1(KOMP)Vlcg}$) mice were purchased from the KOMP repository (VG10108). This mouse line was made by the insertion of a LacZ cassette with a stop codon in the first two exons of *Gpr158* (Orlandi et al., 2015). *Gpr158* conditional allele generation strategy is described in Fig. S3 A. *Gpr158f/f* were generated using 129/Sv embryonic stem cells. Chimeric mice harboring a mutant allele of *Gpr158* were crossed with C57BL/6J WT, and *Gpr158f/+* mice were then crossed with *CamkIIa-Cre* (T29-1; Jax: *B6.Cg-Tg[Camk2a-cre]T29-1Stl/J*) to obtain F2 generation. Analyses of *Gpr158*$_{CamkIIa\text{-}Cre}$ were performed with *Gpr158f/f* as a control. Three-, 12-, and 16-mo-old 129S6/

Map2 in brain slices of 3-mo-old *Gpr158*−/− mice. The right-most panel is a 40× magnification of the region indicated in the middle panel. Bar, 50 µm. (G) Immunofluorescence of Gpr158, Map2, and Gfap in primary hippocampal neuronal preparation. Bar, 50 µm. (H) Gpr158 and serotonin receptor 2C (SR2C) accumulation in *Ocn*−/− and WT hippocampi. Na,K ATPase channel was used as a loading control (Student's *t* test, *n* = 4 mice per group). (I) Bioactive OCN content in the serum of 3-mo-old *Gpr158*−/− (*n* = 4) and WT (*n* = 5 mice; Student's *t* test). (J) Immunofluorescence of c-Fos 1 h after stereotaxic injection of either saline or OCN (10 ng) into the anterior hippocampus of 3-mo-old *Gpr158*−/− and WT mice. Bar, 50 µm. (K) Pull-down assay using biotinylated-OCN on solubilized *Ocn*−/− or *Gpr158*−/− hippocampal membranes. Purified proteins were subjected to Western blot analysis using anti-Gpr158 and anti-Gαq antibodies. (L) IP1 accumulation in *Gpr158*−/− and WT hippocampal neurons treated with saline, OCN, or glutamate as a positive control for 1 h (Student's *t* test, *n* = 12). Results are given as mean ± SEM. *, P ≤ 0.05; **, P ≤ 0.01; ***, P ≤ 0.001.

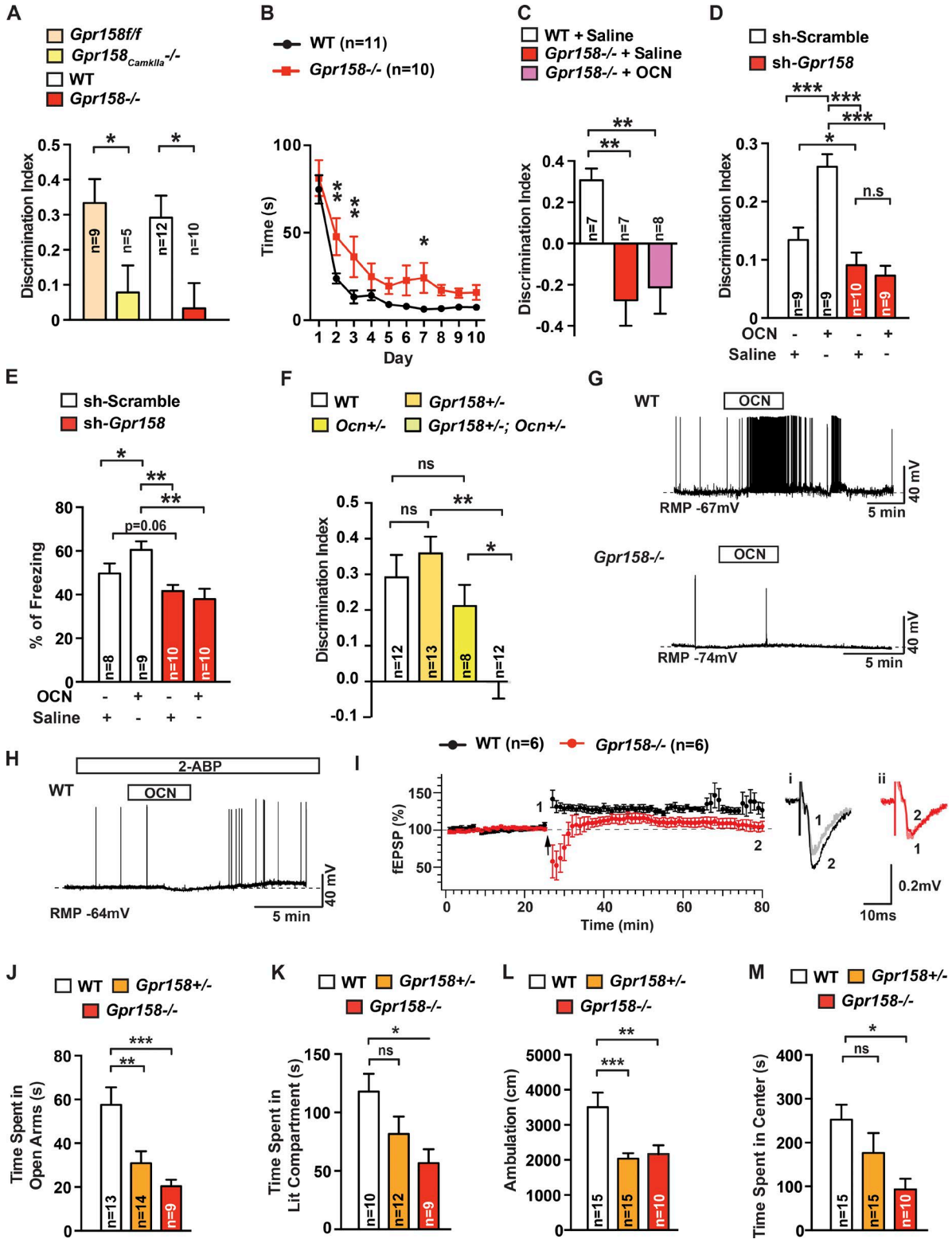

Figure 3. **Functional evidence that OCN signals through Gpr158.** (A) NOR performed in 3-mo-old *Gpr158f/f* (n = 9), *Gpr158*$_{Camklla}$*−/−* (n = 5), *Gpr158−/−* (n = 10), and WT (n = 12) littermates. Discrimination index was measured (Student's t test). (B) MWMT performed in 3-mo-old *Gpr158−/−* (n = 10) and WT (n = 9) littermates. The graph shows the time needed to localize a submerged platform in the swimming area (two-way repeated-measures ANOVA followed by Fisher's least significantly different [LSD] post hoc test). (C) NOR performed in 4-mo-old WT (n = 7) or *Gpr158−/−* mice treated with saline (n = 7) or OCN (n = 8; 90 ng/hr) for 1 mo. Discrimination index was measured (one-way ANOVA compared with WT followed by Bonferroni's post hoc test).

SvEvTac mice were purchased from Taconic Biosciences. Eighteen-mo-old C57BL/6J were obtained from the National Institute on Aging. Upon arrival at the animal facility, mice were housed at least 2 wk before experiments were performed. *Gpr158*+/−, *Ocn*+/−, and *Gpr158*+/−;*Ocn*+/− and *Gpr158*−/− were maintained on a 129-Sv/C57BL/6J mixed genetic background. *Ocn*−/− mice were maintained on a 129-Sv background. Mice were housed five animals per cage (polycarbonate cages, 35.5 × 18 × 12.5 cm), under a 12-h light/dark cycle with ad libitum access to food and water before experimentation. All experiments involving animals were approved by the Institutional Animal Care and Use Committee of Columbia University Medical Center and by the European Communities Council Directive (2010/63/UE).

Primary hippocampal culture

Hippocampal neurons were isolated from mouse embryos (embryonic day 16.5). After dissection, hippocampi were digested with trypsin 0.05% and EDTA 0.02% for 15 min at 37°C. After three washes with DMEM (containing high glucose and sodium pyruvate) supplemented with 10% FBS, 100 U/ml penicillin-streptomycin and 1× GlutaMAX, cells were dissociated by pipetting up and down, and then plated. After the culture was established, culture medium (Neurobasal medium [21103-049; Thermo Fisher Scientific] supplemented with B-27 supplement [17504044; Thermo Fisher Scientific] and 1× GlutaMAX [35050061; Thermo Fisher Scientific]) was changed two times per week. Experiments were performed on cells after 15 d of culture.

Plasma collection

Pooled mouse plasma was collected from 3-mo-old WT or *Ocn*−/− mice or 16-mo-old WT mice by intracardial bleed at time of euthanasia. Plasma was prepared from blood collected with EDTA into Capiject (T-MQK; Terumo) tubes followed by centrifugation at 1,000 *g* for 10 min. All plasma aliquots were stored at −80°C until use. Before administration, plasma was dialyzed using 3.5-kD D-tube dialyzers (71508-3; EMD Millipore) in PBS to remove EDTA. Mice were systemically treated with plasma (100 µl per injection) by injections into the tail vein eight times over 24 d before behavioral analysis. For Western blot analysis, mice were sacrificed to collect hippocampi 4 h after a single plasma injection.

Immunodepletion of OCN from plasma

To remove OCN from plasma derived from 6–12-wk-old mice, anti-C-terminal OCN antibody (Ferron et al., 2010b) or goat control IgG (R&D Systems) was conjugated to 2.8-µm superparamagnetic M-270 Epoxy Dynabeads according to the manufacturer's instructions (Thermo Fisher Scientific), with a coupling ratio of 7 µg of antibody per 1 mg of beads. Covalent conjugation was done at 37°C for 24 h with end-over-end rotation. Coupled beads were washed with PBS before incubation with plasma to prevent detergent contamination. Plasma pooled from 6–12-wk-old female C57BL/6J mice was incubated with beads coupled either to anti-C-terminal OCN antibody or goat control IgG at 4°C overnight with end-over-end rotation, after which the plasma was dialyzed, aliquoted, and kept frozen at −80°C until use. An aliquot of plasma treated with either anti-C-terminal OCN antibody or goat control IgG was analyzed using an OCN ELISA to confirm significant reduction of OCN in the immunodepleted plasma.

Osmotic pumps

Alzet micro-osmotic pumps (model 1002) were loaded with saline or uncarboxylated OCN (30 ng/hr for 12-mo-old and 90 ng/hr for 16-mo-old mice). Mice were anesthetized with isoflurane, and osmotic pumps were surgically installed subcutaneously in the backs of the mice for 28 d.

Gene expression analysis by quantitative PCR

All dissections were performed in ice-cold PBS 1× under a Leica MZ8 dissecting light microscope. All parts of the brain isolated were snap frozen in liquid nitrogen and kept at −80°C until use. Total RNA was isolated from brain tissue and hippocampal cells using TRIZOL (Invitrogen). Total RNA were

(D and E) NOR (D) and contextual fear conditioning (CFC; E) performed in 3-mo-old shRNA scramble- or shRNA *Gpr158*-injected mice. After a 10-d recovery, mice were injected with saline (n = 8–10) or OCN (10 ng; n = 9 or 10). For NOR, discrimination index was measured; for CFC, percentage freezing 24 h after training was measured (two-way repeated-measures ANOVA followed by Fisher's LSD post hoc test). (F) NOR performed in 3-mo-old *Gpr158*+/−;*Ocn*+/− (n = 12), *Ocn*+/− (n = 8), and *Gpr158*+/− (n = 13) littermates. Discrimination index was measured for each group (one-way ANOVA followed by Tukey's post hoc test). (G) OCN's influence on spontaneous action potential (AP) frequency in WT or *Gpr158*−/− CA3 pyramidal neurons (n = 6). The bars above recording traces indicate the application of OCN (10 ng/ml). RMP, resting membrane potential. (H) OCN's effect on spontaneous AP frequency in WT CA3 pyramidal neurons pretreated with 2-aminoethoxydiphenyl borate (2-ABP; n = 4). The bars above the recording traces indicate the application of OCN (10 ng/ml) and 2-ABP (50 µM). (I) LTP in the MF-CA3 synapse from WT and *Gpr158*−/− (Student's t test, n = 6) hippocampal slices. Left: the time course of field excitatory postsynaptic currents (fEPSCs) recorded extracellularly in the CA3 area with a bipolar electrode placed in the mossy fiber (MF) from WT or *Gpr158*−/− slices. Two trains of tetanic stimulation (arrow) were applied to the MF-CA3 synapse (100 Hz, 1-s duration, and 10-s interval) once a stable baseline of fEPSC was recorded. Representative traces of fEPSPs recorded from WT (i) and *Gpr158*−/− slices (ii). Traces recorded before (1) and 50 min after (2) two trains of tetanic stimulations. (J–M) EPMT, dark-to-light transition test (DLT), and OFT performed in 3-mo-old *Gpr158*−/− (n = 9–10), *Gpr158*+/− (n = 12–15), and WT (n = 13–15) littermates. For EPMT, time spent in the open arms was scored; for DLT, time spent in the lit compartment was measured; for OFT, total ambulation and time spent in the center of the arena were measured (one-way ANOVA compared with WT followed by Bonferroni's post hoc test). Results are given as mean ± SEM. *, $P \leq 0.05$; **, $P \leq 0.01$; ***, $P \leq 0.001$.

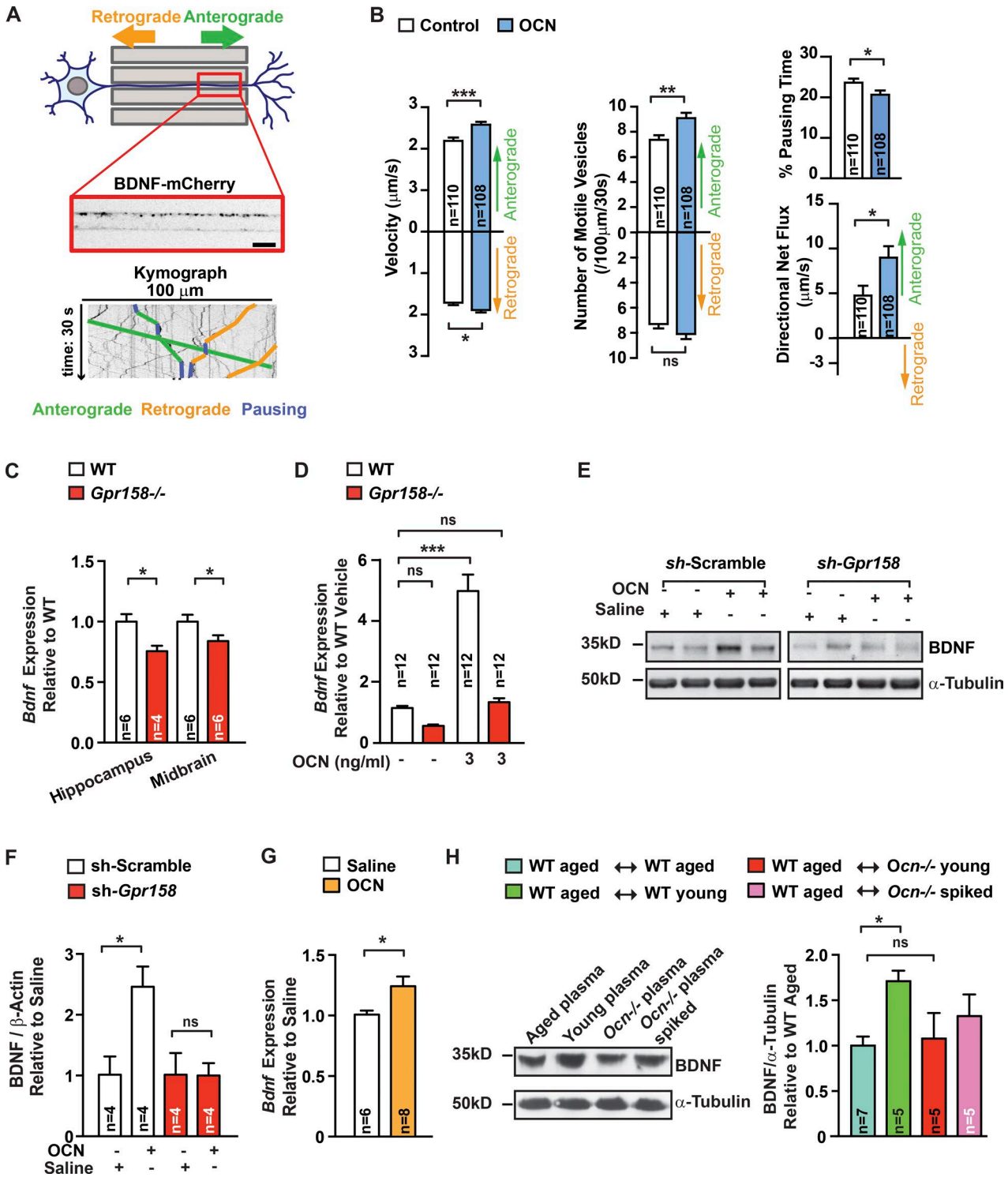

Figure 4. **BDNF as a mediator of OCN function in the brain.** (A) Representation of the microfluidic device (top) composed of somatic and synaptic chambers connected by 500-µm-long microchannels. BDNF-mCherry-positive vesicles were imaged in a 100-µm-long distal region of axons for 30 s. Kymographs (bottom) extracted from the movies. Examples of traces of anterograde (green), retrograde (orange), and pausing (blue) vesicles are depicted on the kymograph. Bar, 10 µm. (B) Quantification of BDNF-mCherry transport in axons of hippocampal neurons cultured in microchambers treated with OCN (n = 108) or vehicle (n = 110) for 4 h (Mann-Whitney U test) compared with control condition. Anterograde and retrograde mean velocities of vesicles per axon, the number of anterograde and retrograde vesicles that are motile in a 100-µm length of axon during 30 s, the percentage of time spent by vesicles in pause, and the directional flux of vesicles within axons were measured. (C and D) *Bdnf* expression (quantitative PCR [qPCR]) in midbrain and hippocampi

first incubated with DNase I for 30 min at room temperature to remove any genomic DNA. DNase I-treated total RNA were converted to cDNA by using M-MLV reverse transcription (28025013; Thermo Fisher Scientific) and random hexamers (N8080127; Thermo Fisher Scientific). Quantitative PCR was performed on a CFX96 Touch Real-Time PCR Detection System (Bio-Rad), and analyses were done using specific quantitative PCR primers and expressed relative to *Gapdh* levels. Quantitative PCR primer sequences for *Gpr158* were as follows: forward, 5′-GCTCATCCTGTT GGAAACAAT-3′; reverse, 5′-TGGCTCAAAGTACAG AATAACGAC-3′; *Bdnf*: forward, 5′-AGTCTCCAGGAC AGCAAAGC-3′; reverse, 5′-TGCAACCGAAGTATGAAA TAACC-3′; *Gapdh*: forward, 5′-AACATCCATCGCGGT CTC-3′; reverse, 5′-CCATTTTGTCTACGGGACGA-3′; and *Gprc6a*: forward, 5′-GGGTTCCTAAAATACCGGACT GC-3′; reverse, 5′-TGCAGTGCATTCATAACTCACC-3′.

In situ hybridization

In situ hybridization was performed on cryosections from tissue fixed with 4% PFA and using 35S-labeled riboprobe as previously described (Ducy et al., 1997). The sequence of *Th*, *Gpr158*, *Gprc6a*, *Gpr156*, *Gpr179*, *Gprc5a*, *Gprc5b*, *Gprc5c*, and *Gprc5d* probe are 500-bp to 1-kb fragments of each gene's 3′ UTR. Hybridizations were performed overnight at 58°C, and washes were performed at 63°C.

Hormonal and second messenger measurement

Circulating levels of OCN in mouse serum were determined with a specific ELISA previously described (Ferron et al., 2010a,b). Total levels of OCN and carboxylated OCN were estimated using two different specific antibodies. Bioactive OCN was determined by subtracting the carboxylated OCN levels from total OCN levels (Ferron et al., 2010a,b). cAMP accumulation was measured by using the cAMP Parameter Assay kit (50-900-648; R&D Systems) and performed in primary hippocampal neurons following the manufacturer's instructions. IP1 accumulation was determined in primary hippocampal neurons by using the IP-One ELISA assay kit (KGE002B; Cisbio) following the manufacturer's instructions. Results are calculated by dividing the optical density of the treated cells by that of the untreated cells and expressed as a percentage of stimulation according the manufacturer's recommendations.

Recombinant OCN

Mouse uncarboxylated OCN was purified from BL21 transformed with pGEX2TK-mOCN as previously described (Lee et al., 2007; Ferron et al., 2010a; Oury et al., 2011, 2013; Mera et al., 2016). In brief, GST-OCN fusion protein was bacterially produced in BL21 pLyS transformed with pGEX-2TK-mOCN after induction with IPTG. Cells were collected in lysis buffer (PBS 1×, 10 mM Tris, pH 7.2, 2 mM EDTA, 1% Triton, and 1× protease and phosphatase inhibitor cocktail; 78443; Thermo Fisher Scientific). Following four freeze-thaw cycles and sonication, lysates were cleared by centrifugation. The supernatant was incubated with glutathione-Sepharose 4B (17075601; GE) for 4 h at 4°C. Following six washes with washing buffer (PBS 1× and 1% Triton) and with PBS 1×, OCN was then cleaved out from the GST moiety by using thrombin (27-0846-01; GE). Four fractions were collected, and each of them was incubated with benzamidine Sepharose (17-5123-10; GE) for 30 min at room temperature to remove thrombin.

Immunoblotting

Frozen hippocampi were pulverized in lysis buffer (20 mM Tris-HCl, pH 7.65, 150 mM NaCl, 1 mM EDTA, 1 mM EGTA, and 1% Triton) supplemented with 1× protease and phosphatase inhibitor cocktail (78443; Thermo Fisher Scientific). Lysates were clarified by centrifugation, and protein concentration was determined using a Bradford assay. Clarified samples were heated at 65°C in Laemmli buffer for 5 min. Proteins were run on an SDS-PAGE gel and transferred to nitrocellulose membrane (1620112; Bio-Rad). Membranes were blocked with TBST-5% BSA for 1 h, incubated with primary antibody overnight at 4°C, and probed with HRP-conjugated antibodies for 1 h at room temperature. The following antibodies were used in these studies: anti-TIMP2 (1:1,000; D18B7; Cell Signaling), anti–α-tubulin (1:5,000; T6199; Sigma-Aldrich), anti-b2 microglobulin (1:1,000; ab75853; Abcam), antitransferrin (1:1,000; ab82411; Abcam), anti-Gpr158 (1:1,000; ABIN486340; Antibodies-online), anti-Na,K ATPase (1:1,000; 3010S; Cell Signaling), anti-SR2C (1:1,000; sc-17797; Santa Cruz), anti-Gaq (1:1,000; D5V1B; Cell Signaling), anti-BDNF (1:100; sc-65514; Santa Cruz). Band intensities were quantified using ImageJ software. Dashed lines separating two bands indicate that these bands are on the same membrane but are not adjacent.

of 6-mo-old *Gpr158*−/− (n = 4–6) and WT (n = 6) littermates (Student's t test; C) and in *Gpr158*−/− and WT hippocampal neurons (one-way ANOVA compared with vehicle-treated cells followed by Bonferroni's post hoc test, n = 12) treated with either saline or OCN for 4 h (D). (E and F) BDNF accumulation (representative Western blot, E) and quantification of band intensities in hippocampi of 3-mo-old shRNA scramble- or shRNA *Gpr158*-injected (F). After a 10 d-long recovery, mice were injected with saline or OCN (10 ng) 16 h before collections (two-way repeated-measures ANOVA followed by Fisher's least significantly different post hoc test, n = 4 per group). (G) *Bdnf* expression (qPCR) in hippocampi of 16-mo-old WT mice injected i.p. with either saline (n = 6) or OCN (n = 8; 500 ng/g BW) 2 h before collection (Student's t test). (H) BDNF accumulation (representative Western blot, left) and quantification of band intensities (right) in hippocampi of older WT mice receiving plasma from older (n = 7) or young WT (n = 5) mice, from young *Ocn*−/− (n = 5) mice, or from young *Ocn*−/− mice supplemented with OCN (n = 5; 90 ng/g BW; one-way ANOVA compared with older WT mice receiving plasma from older WT mice, followed by Bonferroni's post hoc test). α-Tubulin used as a loading control. Results are given as mean ± SEM. *, $P \leq 0.05$; **, $P \leq 0.01$; ***, $P \leq 0.001$.

Immunohistochemistry

Primary cultured neurons were fixed with 4% PFA and 4% sucrose for 20 min and blocked in PBS containing 3% BSA and 0.2% Tween 20 for 2 h at room temperature. Primary antibodies, anti-MAP2 (MAB364; EMD Millipore), anti–glial fibrillary acidic protein (SAB2500462; Sigma-Aldrich), and anti-Gpr158 (ABIN486340; Antibodies-online) were diluted (1:400) in blocking solution and incubated overnight at 4°C. Coverslips were washed three times with PBS 1× containing Triton 0.2%, and secondary antibodies (1:200; Jackson ImmunoResearch) diluted in blocking solution were incubated for 1 h 30 min at room temperature. After three washes, coverslips were mounted with ProLong antifade mountant (Life Technologies). Images were obtained with an inverted Zeiss ApoTome2 microscope. Immunofluorescence of adult brains was performed on 35-µm coronal vibratome slices of tissue fixed with 4% PFA in 0.1 M phosphate buffer. Sections were permeabilized and blocked with 0.5% Triton in TBS, pH 7.4, and 10% normal donkey serum. After blocking, sections were incubated with primary antibodies overnight at 4°C. The following antibodies were used for this assay: anti-c-Fos (1:400; 2250; Cell Signaling), anti-β galactosidase (1:400; ab4761; Abcam), anti-MAP2 (1:1,000; ab5392; Abcam), and anti–glial fibrillary acidic protein (1:400; SAB2500462; Sigma-Aldrich). Sections were washed three times in 0.3% Triton in TBS, pH 7.4, followed by an incubation with secondary antibodies (1:200; Invitrogen) diluted in blocking solution and incubated for 1 h at room temperature. After three washes, sections were mounted with Fluorogel (Electron Microscopy Sciences) and visualized using a Nikon Ti Eclipse microscope. Images were analyzed using ImageJ version 2.0

Pull-down assay

Pulldown of Gpr158 was performed in solubilized membranes from *Ocn*−/− or *Gpr158*−/− hippocampi. Hippocampi were dissected on ice and homogenized in buffer A (10 mM Tris-HCl, pH 7.4, 320 mM sucrose, 1× protease, and phosphatase inhibitor cocktail [78443; Thermo Fisher Scientific]) with a Glass/Teflon Potter Elvehjem homogenizer (20 strokes). Homogenized hippocampi were centrifuged at 3,000 *g* for 10 min at 4°C. Then, supernatants were ultracentrifuged at 40,000 *g* for 20 min at 4°C. Pellets were resuspended in buffer A supplemented with 150 mM NaCl and 1% n-Octyl β-D-thioglucopyranoside (28310; Thermo Fisher Scientific). Solubilized membranes were diluted in buffer A supplemented with 150 mM NaCl and 0.2% n-Octyl β-D-thioglucopyranoside. Recombinant uncarboxylated OCN was biotynalated using the EZ-Link NHS-PEO4 biotynalation kit (21455; Thermo Fisher Scientific) according to the manufacturer's instructions. For the pulldown, biotinylated OCN (7 µg) was incubated for 2 h at 4°C. Thirty microliters of Dynabeads M-280 Streptavidin (11205D; Thermo Fisher Scientific) were added for 30 min at room temperature followed by three PBS 1× washes. Purified proteins were eluted from the beads by adding Laemmli protein buffer and heated at 65°C for 15 min and analyzed by Western blot.

Behavioral tests

All animals of the same batch were born within an interval of 2 wk and were kept in mixed genotype or groups of two to five females in the same cage, at standard laboratory conditions (12-h dark/light cycle, constant room temperature and humidity, and standard laboratory chow and water ad libitum). For each test, mice were transported a short distance from the holding mouse facility to the testing room in their home cages. Behavioral testing was performed between 3 and 16 mo of age, and mouse weight was between 22 and 32 g. The tests were performed by an experimentalist blind to the genotypes or treatment of the mice under study.

EPMT. This test takes advantage of the aversion of rodents to open spaces. The elevated plus maze apparatus comprises two open and two enclosed arms, each with an open roof, elevated 60 cm from the floor (Holmes et al., 2000; Lira et al., 2003). Testing takes place in dim ambient light conditions. Animals are placed into the central area facing one closed arm and allowed to explore the elevated plus maz for 6 min. The total number of arm entries and time spent in open arms is recorded. An increase in anxiety is indicated by a decrease in the proportion of time spent in the open arms (time in open arms/total time in open or closed arms) and a decrease in the proportion of entries into the open arms.

Light–to–dark transition test. This test is based on the innate aversion of rodents to brightly illuminated areas and on their spontaneous exploratory behavior in response to the stressor that light represents. The test apparatus consists of a dark, safe compartment and an illuminated, aversive one. Mice were tested for 6 min, and two parameters were recorded: time spent in the lit compartment and the number of transitions between compartments, indices of anxiety-related behavior and exploratory activity.

OFT. This test takes advantage of the aversion of rodents to brightly lit areas (David et al., 2009). Each mouse is placed in the center of the OFT chamber (a white 43 × 43 cm chamber) and allowed to explore for 30 min. Mice were monitored throughout each test session by video recording and analyzed using autotyping (Patel et al., 2014). The overall motor activity was quantified as the total distance traveled (ambulation). Anxiety was quantified by measuring the time spent in the center of the OFT chamber.

Morris water maze test. Animals were transported to the testing room in their home cages and left undisturbed for at least 30 min before the first trial. The maze was comprised of a large swimming pool (150 cm in diameter) filled with water (23°C) made opaque with nontoxic white paint. The pool was located in a brightly lit room filled with visual cues, in-

cluding geometric figures on the walls of the maze demarking the four fixed starting positions of the trials, at 12 o'clock, 3 o'clock, 6 o'clock, and 9 o'clock. A 15-cm round platform was hidden 1 cm beneath the surface of the water at a fixed position. Each daily trial block consisted of four swimming trials, with each mouse starting from the same randomly chosen starting position. The starting position was varied between days. On day 1, mice that failed to find the platform within 2 min were guided to the platform. They were required to remain on the platform for 15 s before they were returned to their home cages. Mice were not guided to the platform after day 1, and the time it took them to reach the platform over repeated trials (three trials each day for the next 10 d) was recorded as a measure of spatial learning.

NOR test. The NOR paradigm assesses a rodent's ability to recognize a novel object in the environment. The NOR task was conducted, as previously described (Broadbent et al., 2010), in an opaque plastic box using two different objects: (a) a clear plastic funnel (diameter 8.5 cm, maximal height 8.5 cm) and (b) a black plastic box (9.5 cm^3). These objects elicit equal levels of exploration as determined in pilot experiments (Denny et al., 2012; Oury et al., 2013). The NOR paradigm consists of three exposures over the course of 3 d. On day 1, the habituation phase, mice are given 5 min to explore the empty arena, without any objects. On day 2, the familiarization phase, mice are given 10 min to explore two identical objects, placed at opposite ends of the box. On day 3, the test phase, mice are given 15 min to explore two objects, one novel object and a copy of the object from the familiarization phase. The object that serves as the novel object (either the funnel or the box) as well as the left/right starting position of the objects is counterbalanced within each group. Mice are placed in the center of the arena at the start of each exposure. Between exposures, mice are held individually in standard cages, the objects and arenas are cleaned, and the bedding is replaced. Preference for the novel object is assessed on the basis of the fraction of time that a mouse spends exploring the novel object compared with the familiar object. Exploration is scored from video recordings of each exposure and scored using the Stopwatch program. Climbing or sitting adjacent to the object were not counted as exploration. An equal exploration time for the two objects, or a decreased percentage of time spent with the novel object compared with WT controls indicates impairment in hippocampal memory. For this test, discrimination index ([time spent with novel object − time spent with old object]/total exploration time) and preference index (time spent with novel object/total exploration time) were measured.

Contextual fear conditioning. The conditioning apparatus consisted of sound-attenuating conditioning boxes (Bioseb), and mice were run individually in the conditioning boxes. The floor of the chamber consisted of stainless steel bars wired to a shock generator with a scrambler for the delivery of foot shock. Signal generated by mouse movement was recorded and analyzed by a high-sensitivity weight transducer system. The fear-conditioning procedure took place over two consecutive days. On day 1, mice were placed in the conditioning chamber and received three foot shocks (1 s, 0.5 mA), which were administered at time points of 60, 120, and 180 s after the animals were placed in the chamber. They were returned to their home cage 60 s after the final shock. Contextual fear memory was assessed 24 h after conditioning by returning the mice to the conditioning chamber and measuring freezing behavior during a 4-min retention test. Freezing was scored and analyzed automatically using Packwin software version 2.0 (Bioseb). Freezing behavior was considered to occur if the animals froze for a period of at least 2 s.

Electrophysiology

Coronal brain slices containing the hippocampus were prepared from WT and *Gpr158*−/− mice (males, 3–4 wk old), as previously reported (Rao et al., 2007). In brief, mice were anesthetized with isoflurane and then decapitated to harvest brains, which were rapidly removed and immersed in an oxygenated cutting solution at 4°C containing 220 mM sucrose, 2.5 mM KCl, 1 mM $CaCl_2$, 6 mM $MgCl_2$, 1.25 mM NaH_2PO_4, 26 mM $NaHCO_3$, and 10 mM glucose and adjusted to pH 7.3 with NaOH. Coronal slices containing the hippocampus (350 µm thick) were cut with a vibratome and trimmed to contain just the hippocampus. After preparation, slices were stored in a holding chamber at room temperature (22–25°C) with oxygenated (5% CO_2 and 95% O_2) artificial cerebrospinal fluid (ACSF) containing 124 mM NaCl, 3 mM KCl, 2 mM $CaCl_2$, 2 mM $MgCl_2$, 1.23 mM NaH_2PO_4, 26 mM $NaHCO_3$, and 10 mM glucose, pH 7.4, with NaOH. The slices were eventually transferred to a recording chamber continuously perfused with ACSF at 33°C at a rate of 2 ml/min for at least a 1 h to allow recovery before the start of patch-clamp recording. Whole-cell current clamp was performed to observe spontaneous APs in visually identified pyramidal neurons in the CA3 area of the hippocampus, as reported by Kim and Connors (2012), with a Multiclamp 700 A amplifier (Molecular Devices). The patch pipettes with a tip resistance of 4–6 MΩ were made of borosilicate glass (World Precision Instruments) with a pipette puller (Sutter P-97) and back filled with a pipette solution containing 135 mM K-gluconate, 2 mM $MgCl_2$, 10 mM Hepes, 1.1 mM EGTA, 2 mM Mg-ATP, 10 mM Na_2-phosphocreatine, and 0.3 mM Na_2-GTP, pH 7.3, with KOH. After a stable base of APs were recorded for 10 min, OCN was applied to the recorded cells through bath application at a concentration of 10 ng/ml for 10 min and then washed out with ACSF. Both input resistance and series resistance were monitored throughout the experiments. Only recordings with stable series resistance were accepted (the change in series resistance was less than 20%). In LTP experiments, fEPSPs were recorded in the CA3 area with a glass pipette filled with ACSF (with a tip resistance of 2–4 MΩ) by stimulating the MF in the dentate gyrus area

with a bipolar electrode. The amplitude of fEPSPs was always adjusted to 40% of the maximum value before the starting of LTP experiments. Two trains of high-frequency stimuli (100 Hz, 1-s duration, 10-s interval) were delivered to the MF after a stable baseline recording of fEPSPs was achieved, as routinely reported by others (Spillane et al., 1995). The amplitude of fEPSPs was normalized to the mean amplitude of fEPSPs recorded before high-frequency stimulations, as reported by others (Spillane et al., 1995). All data were sampled at 10 kHz and filtered at 6 kHz with an Apple Macintosh computer using Axograph X (AxoGraph Scientific). APs were detected and analyzed with AxoGraph X and plotted with Igor Pro software (WaveMetrics), as described previously (Rao et al., 2007). 2-Aminoethoxydiphenyl borate (1224; Tocris Bioscience) was used to inhibit IP3 receptor.

Lentivirus production and shRNA sequences

The shRNA sequence 5′-GAGCCGCTCCACTGACGG CACCATCTTGG-3′ targeting mouse *Gpr158* was purchased from Origene (TL509693B). shRNA was cloned into pGFP-C-Lentivector (Origene). For virus production, human embryonic kidney 293T cells were transfected with VSVG, helper, and pGFP-C-shLentiVector (containing Gpr158 or scramble shRNA) plasmids. After 2 d, viral particles were purified and concentrated.

Stereotaxic injection

Stereotaxic surgery was performed in 3-mo-old C57BL/6J male mice obtained from the Janvier Laboratory stock. Mice were anesthetized with intraperitoneal injection of a mixture of ketamine hydrochloride (100 mg/kg of body weight [BW]; 1000; Virbac) and 100 mg/ml BW xylazine (10 mg/kg of BW; Rompun 2%; Bayer) and placed in a stereotaxic frame (900SL-KOPF). Ophthalmic eye ointment was applied to the cornea to prevent desiccation during surgery. The fur in the area surrounding the incision was trimmed, and Vetedine solution (Vétoquinol) was applied. Lentiviruses expressing shRNA targeting Gpr158 or noneffective scramble shRNA in pGFP-C-shLentiVector were injected bilaterally into the anterior hippocampi ([from bregma] anteroposterior = −2.0 mm, dorsal ventral = ±1.4 mm, and medial lateral = −1.33 mm) using a 10-µl Hamilton syringe (1701RN) over either 12 or 4 min (injection speed 0.25 µl/min). Three microliters of lentivirus expressing shRNA against *Gpr158* (titer: 3.4 × 10^9 GC/ml) or scramble shRNA (1.4 × 10^9 GC/ml) were injected. To limit reflux along the injection track, the needle was maintained in place for 4 min between each 1-µl injection. Then, the skin was closed using silk suture and the mice were injected locally with surgical analgesic (ketoprofen). Two weeks after the lentivirus injection, bilateral stereotaxic injections of OCN (10 ng/µl) or NaCl was performed into the anterior hippocampi at the same stereotaxic coordinate. Twelve hours after the stereotaxic injections of OCN, mice were subjected to the training phase (NOR and contextual fear conditioning) and to the testing phase 24 h following the habituation phase.

Live-cell imaging of BDNF axonal trafficking in microfluidic devices

Primary hippocampal neurons were prepared from E17.5 WT rats. Dissociated neurons were resuspended in growing medium (Neurobasal medium supplemented with 2% B27, 2 mM Glutamax, and 1% penicillin/streptomycin) and seeded in the upper chamber of microchambers prepared according to Zala et al. (2013) at a final density of 7,000 cells/mm^2. Three hours after seeding, neurons were infected with 3.10^5 UI of lentivirus carrying pCMV-BDNF-mCherry constructs and cultured for 9 to 11 d at 37°C in a 5% CO_2 incubator. Neurons were treated or not for 4 h with 10 ng/ml OCN added in the upper chamber and imaged. Videomicroscopy acquisitions of 100-µm axon length were done on the lower part of channels, far enough from dendrites, at 5 Hz for 30 s with an inverted microscope (AxioObserver Z1; Zeiss) coupled to a spinning-disk confocal system (CSU-W1-T3; Yokogawa) connected to an electron-multiplying charge-coupled device camera (ProEM$^+$1024; Princeton Instrument) at 37°C and 5% CO_2. BDNF-mCherry positive mean vesicle velocity per axon, vesicle number per 100 µm length axon over 30 s, percentage of vesicle pausing time, and directional net flux (mean velocity × number of anterograde vesicles per axon − mean velocity × number of retrograde vesicles per axon) were extracted from kymographs (x axis, 100 µm; y axis, 30 s) using the KymoTool Box ImageJ plugin as previously described (Zala et al., 2013). Each condition was tested using 3 microchambers per culture and three independent cultures. In each chamber, three fields containing at least four axons were analyzed to reach a minimum number of 100 axons (1,400 vesicles).

Quantification and statistical analysis

All values are expressed as mean ± SEM. Statistical parameters including the exact sample size (n), post hoc tests, and statistical significance are reported in every figure and figure legend. Number of mice were estimated to be sufficient on the basis of pilot experiments and previously published work (Oury et al., 2013). Data were estimated to be statistically significant when $P \leq 0.05$ by nonparametric Mann-Whitney *U* test, Student's *t* test, one-way ANOVA, or two-way ANOVA. In every figure, an asterisk denotes statistical significance (*, $P \leq 0.05$; **, $P \leq 0.01$; ***, $P \leq 0.001$). Data were analyzed using GraphPad Prism 6.

Online supplemental material

Fig. S1 shows bioactive OCN levels in various animal models, as well as the peripheral treatment of 12-mo-old mice with OCN. Fig. S2 shows the negative control for the expression pattern of all class C orphan family GPCRs in the hippocampal region and the stereotactic coordinates used for hip-

pocampal injections. Fig. S3 presents how the brain-specific deletion of Gpr158 was performed.

ACKNOWLEDGMENTS

We thank Drs. P. Ducy and E. Passegue for critical reading of the manuscript.

This work was supported by National Institute on Aging grant 2P01 AG032959-06A1 and the Columbia Aging Center (G. Karsenty), National Institute of Diabetes and Digestive and Kidney Diseases Endocrinology Training Grant 5T32DK007328-38 (L. Khrimian), Fondation pour la Recherche Médicale grant AJE20130928594, a Career Development Award from the Human Frontier Scientific Program, ATIP-AVENIR Program of Institut National de la Santé et de la Recherche Médicale (F. Oury), the AGEMED Program of Institut National de la Santé et de la Recherche Médicale (F. Oury and F. Saudou), and the Philippe Foundation (A. Obri).

The authors declare no competing financial interests.

Author contributions: L. Khrimian, A. Obri, F. Oury, E. Kandel, and G. Karsenty designed experiments. L. Khrimian, A. Obri, M. Ramos-Brossier, A. Rousseaud, S. Moriceau, P. Mera, X.-B. Gao, T. Karnavas, A.-S. Nicot, F. Saudou, and S. Kosmidis performed experiments. L. Khrimian, A. Obri, F. Oury, and G. Karsenty analyzed data. L. Khrimian, A. Obri, F. Oury, and G. Karsenty wrote the manuscript.

Submitted: 25 July 2017
Revised: 1 August 2017
Accepted: 3 August 2017

REFERENCES

Broadbent, N.J., S. Gaskin, L.R. Squire, and R.E. Clark. 2010. Object recognition memory and the rodent hippocampus. *Learn. Mem.* 17:5–11. http://dx.doi.org/10.1101/lm.1650110

Castellano, J.M., K.I. Mosher, R.J. Abbey, A.A. McBride, M.L. James, D. Berdnik, J.C. Shen, B. Zou, X.S. Xie, M. Tingle, et al. 2017. Human umbilical cord plasma proteins revitalize hippocampal function in aged mice. *Nature.* 544:488–492. http://dx.doi.org/10.1038/nature22067

Chiappe, A., G. Gonzalez, E. Fradinger, G. Iorio, J.L. Ferretti, and J. Zanchetta. 1999. Influence of age and sex in serum osteocalcin levels in thoroughbred horses. *Arch. Physiol. Biochem.* 107:50–54. http://dx.doi.org/10.1076/apab.107.1.50.4357

Crawley, J.N. 1985. Exploratory behavior models of anxiety in mice. *Neurosci. Biobehav. Rev.* 9:37–44. http://dx.doi.org/10.1016/0149-7634(85)90030-2

David, D.J., B.A. Samuels, Q. Rainer, J.W. Wang, D. Marsteller, I. Mendez, M. Drew, D.A. Craig, B.P. Guiard, J.P. Guilloux, et al. 2009. Neurogenesis-dependent and -independent effects of fluoxetine in an animal model of anxiety/depression. *Neuron.* 62:479–493. http://dx.doi.org/10.1016/j.neuron.2009.04.017

Denny, C.A., N.S. Burghardt, D.M. Schachter, R. Hen, and M.R. Drew. 2012. 4- to 6-week-old adult-born hippocampal neurons influence novelty-evoked exploration and contextual fear conditioning. *Hippocampus.* 22:1188–1201. http://dx.doi.org/10.1002/hipo.20964

Ducy, P., C. Desbois, B. Boyce, G. Pinero, B. Story, C. Dunstan, E. Smith, J. Bonadio, S. Goldstein, C. Gundberg, et al. 1996. Increased bone formation in osteocalcin-deficient mice. *Nature.* 382:448–452. http://dx.doi.org/10.1038/382448a0

Ducy, P., R. Zhang, V. Geoffroy, A.L. Ridall, and G. Karsenty. 1997. Osf2/Cbfa1: a transcriptional activator of osteoblast differentiation. *Cell.* 89:747–754. http://dx.doi.org/10.1016/S0092-8674(00)80257-3

Ferron, M., J. Wei, T. Yoshizawa, A. Del Fattore, R.A. DePinho, A. Teti, P. Ducy, and G. Karsenty. 2010a. Insulin signaling in osteoblasts integrates bone remodeling and energy metabolism. *Cell.* 142:296–308. http://dx.doi.org/10.1016/j.cell.2010.06.003

Ferron, M., J. Wei, T. Yoshizawa, P. Ducy, and G. Karsenty. 2010b. An ELISA-based method to quantify osteocalcin carboxylation in mice. *Biochem. Biophys. Res. Commun.* 397:691–696. http://dx.doi.org/10.1016/j.bbrc.2010.06.008

Hall, J., K.L. Thomas, and B.J. Everitt. 2000. Rapid and selective induction of BDNF expression in the hippocampus during contextual learning. *Nat. Neurosci.* 3:533–535. http://dx.doi.org/10.1038/75698

Holmes, A., S. Parmigiani, P.F. Ferrari, P. Palanza, and R.J. Rodgers. 2000. Behavioral profile of wild mice in the elevated plus-maze test for anxiety. *Physiol. Behav.* 71:509–516. http://dx.doi.org/10.1016/S0031-9384(00)00373-5

Kamiya, H., H. Shinozaki, and C. Yamamoto. 1996. Activation of metabotropic glutamate receptor type 2/3 suppresses transmission at rat hippocampal mossy fibre synapses. *J. Physiol.* 493:447–455. http://dx.doi.org/10.1113/jphysiol.1996.sp021395

Karsenty, G., and E.N. Olson. 2016. Bone and muscle endocrine functions: unexpected paradigms of inter-organ communication. *Cell.* 164:1248–1256. http://dx.doi.org/10.1016/j.cell.2016.02.043

Kim, J.A., and B.W. Connors. 2012. High temperatures alter physiological properties of pyramidal cells and inhibitory interneurons in hippocampus. *Front. Cell. Neurosci.* 6:27. http://dx.doi.org/10.3389/fncel.2012.00027

Lee, N.K., H. Sowa, E. Hinoi, M. Ferron, J.D. Ahn, C. Confavreux, R. Dacquin, P.J. Mee, M.D. McKee, D.Y. Jung, et al. 2007. Endocrine regulation of energy metabolism by the skeleton. *Cell.* 130:456–469. http://dx.doi.org/10.1016/j.cell.2007.05.047

Lira, A., M. Zhou, N. Castanon, M.S. Ansorge, J.A. Gordon, J.H. Francis, M. Bradley-Moore, J. Lira, M.D. Underwood, V. Arango, et al. 2003. Altered depression-related behaviors and functional changes in the dorsal raphe nucleus of serotonin transporter-deficient mice. *Biol. Psychiatry.* 54:960–971. http://dx.doi.org/10.1016/S0006-3223(03)00696-6

Maruyama, T., T. Kanaji, S. Nakade, T. Kanno, and K. Mikoshiba. 1997. 2APB, 2-aminoethoxydiphenyl borate, a membrane-penetrable modulator of Ins(1,4,5)P3-induced Ca2+ release. *J. Biochem.* 122:498–505. http://dx.doi.org/10.1093/oxfordjournals.jbchem.a021780

Mera, P., K. Laue, M. Ferron, C. Confavreux, J. Wei, M. Galán-Díez, A. Lacampagne, S.J. Mitchell, J.A. Mattison, Y. Chen, et al. 2016. Osteocalcin signaling in myofibers is necessary and sufficient for optimum adaptation to exercise. *Cell Metab.* 23:1078–1092. http://dx.doi.org/10.1016/j.cmet.2016.05.004

Nakazawa, K., M.C. Quirk, R.A. Chitwood, M. Watanabe, M.F. Yeckel, L.D. Sun, A. Kato, C.A. Carr, D. Johnston, M.A. Wilson, and S. Tonegawa. 2002. Requirement for hippocampal CA3 NMDA receptors in associative memory recall. *Science.* 297:211–218. http://dx.doi.org/10.1126/science.1071795

Orlandi, C., K. Xie, I. Masuho, A. Fajardo-Serrano, R. Lujan, and K.A. Martemyanov. 2015. Orphan receptor GPR158 is an allosteric modulator of RGS7 catalytic activity with an essential role in dictating its expression and localization in the brain. *J. Biol. Chem.* 290:13622–13639. http://dx.doi.org/10.1074/jbc.M115.645374

Oury, F., G. Sumara, O. Sumara, M. Ferron, H. Chang, C.E. Smith, L. Hermo, S. Suarez, B.L. Roth, P. Ducy, and G. Karsenty. 2011. Endocrine regulation of male fertility by the skeleton. *Cell.* 144:796–809. http://dx.doi.org/10.1016/j.cell.2011.02.004

Oury, F., L. Khrimian, C.A. Denny, A. Gardin, A. Chamouni, N. Goeden, Y.Y. Huang, H. Lee, P. Srinivas, X.B. Gao, et al. 2013. Maternal and offspring pools of osteocalcin influence brain development and functions. *Cell.* 155:228–241. http://dx.doi.org/10.1016/j.cell.2013.08.042

Patel, T.P., D.M. Gullotti, P. Hernandez, W.T. O'Brien, B.P. Capehart, B. Morrison III, C. Bass, J.E. Eberwine, T. Abel, and D.F. Meaney. 2014. An open-source toolbox for automated phenotyping of mice in behavioral tasks. *Front. Behav. Neurosci.* 8:349. http://dx.doi.org/10.3389/fnbeh.2014.00349

Rao, Y., Z.W. Liu, E. Borok, R.L. Rabenstein, M. Shanabrough, M. Lu, M.R. Picciotto, T.L. Horvath, and X.B. Gao. 2007. Prolonged wakefulness induces experience-dependent synaptic plasticity in mouse hypocretin/orexin neurons. *J. Clin. Invest.* 117:4022–4033. http://dx.doi.org/10.1172/JCI32829

Saxe, M.D., F. Battaglia, J.W. Wang, G. Malleret, D.J. David, J.E. Monckton, A.D. Garcia, M.V. Sofroniew, E.R. Kandel, L. Santarelli, et al. 2006. Ablation of hippocampal neurogenesis impairs contextual fear conditioning and synaptic plasticity in the dentate gyrus. *Proc. Natl. Acad. Sci. USA.* 103:17501–17506. http://dx.doi.org/10.1073/pnas.0607207103

Smith, L.K., Y. He, J.S. Park, G. Bieri, C.E. Snethlage, K. Lin, G. Gontier, R. Wabl, K.E. Plambeck, J. Udeochu, et al. 2015. β2-microglobulin is a systemic pro-aging factor that impairs cognitive function and neurogenesis. *Nat. Med.* 21:932–937. http://dx.doi.org/10.1038/nm.3898

Spillane, D.M., T.W. Rosahl, T.C. Südhof, and R.C. Malenka. 1995. Long-term potentiation in mice lacking synapsins. *Neuropharmacology.* 34:1573–1579. http://dx.doi.org/10.1016/0028-3908(95)00107-H

Villeda, S.A., K.E. Plambeck, J. Middeldorp, J.M. Castellano, K.I. Mosher, J. Luo, L.K. Smith, G. Bieri, K. Lin, D. Berdnik, et al. 2014. Young blood reverses age-related impairments in cognitive function and synaptic plasticity in mice. *Nat. Med.* 20:659–663. http://dx.doi.org/10.1038/nm.3569

Yamada, K., and T. Nabeshima. 2003. Brain-derived neurotrophic factor/TrkB signaling in memory processes. *J. Pharmacol. Sci.* 91:267–270. http://dx.doi.org/10.1254/jphs.91.267

Zala, D., M.V. Hinckelmann, H. Yu, M.M. Lyra da Cunha, G. Liot, F.P. Cordelières, S. Marco, and F. Saudou. 2013. Vesicular glycolysis provides on-board energy for fast axonal transport. *Cell.* 152:479–491. http://dx.doi.org/10.1016/j.cell.2012.12.029